Proceedings of the ASME 2010 3rd Joint US-European Fluids Engineering Summer Meeting and 8th International Conference on Nanochannels, Microchannels, and Minichannels
FEDSM-ICNMM2010
August 1-5, 2010, Montreal, Canada

FEDSM-ICNMM2010-30572

UNCERTAINTY QUANTIFICATION OF TURBULENCE MODEL COEFFICIENTS VIA LATIN HYPERCUBE SAMPLING METHOD

Matthew C. Dunn
Department of
Mechanical & Aerospace Engineering
The University of Alabama in Huntsville
Huntsville, Alabama 35899
mcd0002@uah.edu

Babak Shotorban*
Department of
Mechanical & Aerospace Engineering
University of Alabama in Huntsville
Huntsville, Alabama 35899
babak.shotorban@uah.edu

Abdelkader Frendi
Department of
Mechanical & Aerospace Engineering
University of Alabama in Huntsville
Huntsville, Alabama 35899
kader.frendi@uah.edu

ABSTRACT

This paper is concerned with the propagation of uncertainties in the values of turbulence model coefficients and parameters in turbulent flows. These coefficients and parameters are determined from experiments performed on elementary flows and they are subject to uncertainty. The widely used $k-\varepsilon$ turbulence model is considered. It consists of model transport equations for the turbulence kinetic energy and rate of turbulent dissipation. Both equations involve various model coefficients about which adequate knowledge is assumed known in the form of probability density functions. The study is carried out for the flow over a 2D backward-facing step configuration. The Latin Hypercube Sampling method is employed for the uncertainty quantification purposes as it requires a smaller number of samples compared to the conventional Monte-Carlo method. The mean values are reported for the flow output parameters of interest along with their associated uncertainties. The results show that model coefficient variability has significant effects on the streamwise velocity component in the recirculation region near the reattachment point and turbulence intensity along the free shear layer. The reattachment point location, pressure, and wall shear are also significantly affected.

NOMENCLATURE

A_1 beta distribution parameter
A_2 beta distribution parameter
B wall function parameter
$C_{\varepsilon 1}$ $k-\varepsilon$ model constant
$C_{\varepsilon 2}$ $k-\varepsilon$ model constant
C_μ $k-\varepsilon$ model constant
C_f friction coefficient
C_{fout} fully developed friction coefficient
C_p pressure coefficient
G kernal density bandwidth
h step height
h_i backward-facing step inlet height
H backward-facing step channel height
I_T nondimensional turbulence intensity
K kernal
k_0 turbulence kinetic energy at reference time
k turbulence kinetic energy
L_c backward-facing step channel length
L_i backward-facing step inlet length
n decay rate
N number of samples
p beta distribution parameter
P rate of production of turbulent kinetic energy
P_0 centerline inlet pressure
q beta distribution parameter
Re Reynolds number
S mean shear rate
t time
U inlet velocity
U_i Reynolds-averaged velocity component in i direction

*Address all correspondence to this author.

U_0 centerline inlet velocity
u_i fluctuation of the velocity component in i direction
u_τ local wall-shear velocity
x_r reattachment point
y^+ distance from the wall

Greek

α_w Weibull distribution shape parameter
β_w Weibull distribution scale parameter
δ kronecker delta
ε_0 dissipation rate at reference time
ε dissipation rate
κ von Kármán constant
μ mean
μ_l lognormal mean
μ_f dynamic viscosity
ν kinematic viscosity
ν_T turbulent viscosity
ρ density
σ_l lognormal standard deviation
σ standard deviation
σ_k $k-\varepsilon$ model constant
σ_ε $k-\varepsilon$ model constant
τ turbulence time scale
τ_w wall shear stress

INTRODUCTION

Until recently, computational fluid dynamics (CFD) analysis methods have been entirely deterministic meaning that single values of the input variables and physical constants are used to calculate single estimates of the fluid flow behavior. However, in reality the input data are not known exactly and they contain uncertainties [1]. In particular, such uncertainties exist for the coefficients associated with turbulence model which are available for the CFD analysis of turbulent flows.

In order to achieve a numerical solution of a turbulent flow, the Navier-Stokes equations of motion which encompass the physical principles of the conservation of mass and momentum need to be solved. Direct numerical simulations (DNS) of these equations in the case of turbulent flows are currently not feasible for flows with high Reynolds numbers which are of practical interest. The reason is that at high Reynolds numbers, the smallest scales of the flow turbulence compared to the geometrical scale of the flow is so small that resolving all scales is not numerically possible with present computational resources. One commonly used method to overcome this issue is to solve the Reynolds-averaged Navier-Stokes (RANS) equations instead. With the use of these equations new unknown terms arise and warrant the need for additional relations in order to close the system of equations. These relations are built up through turbulence models. Because these turbulence model approximations have been tuned through some coefficients based on elementary experiments, which are statistical processes, uncertainties are inherent in the models. An uncertainty quantification methodology is developed and employed in this paper to study the propagation of these uncertainties in a backward facing step flow. In the context of turbulence, similar studies through other methodologies have been performed by Platteeuw et al. [2] for RANS, and Lucor et al. [3] and Jouhaud et al. [4] for Large-eddy Simulation (LES).

There are various turbulence models available in the literature [5] with the two-equation standard $k-\varepsilon$ model [6] being perhaps the most popular one. The standard $k-\varepsilon$ model can be found in almost all commercial codes utilized for the CFD analysis of turbulent flows. In the current work we assume that there are uncertainties in the values of coefficients used in this model and we make use of available information in the literature about them to construct their probability density functions (PDFs) [7]. We emphasize that this paper does not stand to prove the accuracy of the $k-\varepsilon$ model but is concerned with the uncertainties of the coefficients and subsequent effects of their propagation through the model to flow variables as outputs.

The Latin Hypercube Sampling (LHS) technique [8–10] has been adopted in this work for uncertainty quantification purposes. LHS is a variation of stratified sampling that can be applied to multiple variable optimizations as a method to alleviate the shortcomings of deterministic methods [11, 12]. The LHS method is commonly used to reduce the number of samples necessary in the conventional Monte-Carlo method to achieve a reasonably accurate random distribution [13]. Whereas the conventional Monte-Carlo method picks sampling points at random within the domain, LHS method samples the entire domain in a more systematic manner.

TURBULENCE MODEL DESCRIPTION

The $k-\varepsilon$ turbulence model consists of a model transport equation for the turbulence kinetic energy k and another model transport equation for the turbulence dissipation rate ε. Using Einstein notation these equations, respectively, read [5]

$$\frac{\partial k}{\partial t}+U_i\frac{\partial k}{\partial x_i}=\frac{\partial}{\partial x_j}\left(\frac{\nu_T}{\sigma_k}\frac{\partial k}{\partial x_j}\right)+P-\varepsilon, \tag{1}$$

and

$$\frac{\partial \varepsilon}{\partial t}+U_i\frac{\partial \varepsilon}{\partial x_i}=\frac{\partial}{\partial x_j}\left(\frac{\nu_T}{\sigma_\varepsilon}\frac{\partial \varepsilon}{\partial x_j}\right)+C_{\varepsilon 1}\frac{P\varepsilon}{k}-C_{\varepsilon 2}\frac{\varepsilon^2}{k}. \tag{2}$$

The turbulent viscosity ν_T in Eqs. (1) and (2) is calculated by

$$\nu_T=C_\mu\frac{k^2}{\varepsilon}. \tag{3}$$

Modeling Reynolds stresses $\overline{u_i u_j}$ through the turbulent-viscosity hypothesis [5] by

$$\overline{u_i u_j} = \frac{2}{3} k \delta_{ij} - \nu_T \left(\frac{\partial U_i}{\partial x_j} + \frac{\partial U_j}{\partial x_i} \right), \tag{4}$$

the production term P seen in Eqs. (1) and (2) and defined by

$$P = -\overline{u_i u_j} \frac{\partial U_j}{\partial x_i}, \tag{5}$$

can be calculated.

For applications near the viscous wall, with a considerably lower local Reynolds number, the $k-\varepsilon$ model has been shown to achieve poor results. The reason is that this model is basically derived making a high Reynolds number assumption in the turbulent flow. In order to alleviate the wall issue of the $k-\varepsilon$ model, the use of wall function models along with this model is a commonly practiced. The log law of the wall due to von Kármán [14] is

$$u^+ = \frac{1}{\kappa} \ln y^+ + B, \tag{6}$$

where, κ is the von Kármán constant and the parameter B is an empirical constant as a function of the smoothness of the wall. The log-law relation has been confirmed to hold true for the region $y^+ > 30$ [5].

Values of model constants seen in Eqs. (1-3) are given by Launder and Sharma [15]

$$C_\mu = 0.09,\ C_{\varepsilon 1} = 1.44,\ C_{\varepsilon 2} = 1.92,\ \sigma_k = 1.0,\ \sigma_\varepsilon = 1.3. \tag{7}$$

The influence of uncertainties of these values and those of B and κ seen in Eq. (6) in the flow is the main subject of current study.

PROBABILITY DENSITY FUNCTIONS OF MODEL COEFFICIENTS

In order to quantify the uncertainty in the turbulence model coefficients, their probability density functions are used. There are a total of eight uncertain quantities including five $k-\varepsilon$ model coefficients, two wall function parameters, and the turbulence intensity at the inlet boundary condition. The PDFs for the turbulence model coefficients and wall function parameters are estimated using the data available for them in the literature [5].

In the current work, *EasyFit* sofware, a product of MathWave Technologies, is utilized to estimate the PDF from available data for each uncertain quantity. *EasyFit* proposes various estimated PDFs while ranking them according to the 'goodness of fit' criteria which is measured in terms of the Kolmogorov-Smirnov function [16]. Among the ranked PDFs proposed by *EasyFit*, we choose the one with the highest possible rank which can be given as an input to the LHS software. We use Sandia National Laboratories LHS software in this study and not all types of PDFs outputted by *EasyFit* can be given as inputs to this LHS software .

The probability density function for the coefficient C_μ in Eq. (3) is obtained from statistical correlations made through the comparison of DNS and experimental results of a fully developed turbulent channel flow [17]. The values of this coefficient are extracted from the DNS data by rearranging the turbulent viscosity equation in terms of C_μ

$$C_\mu = \frac{\nu_T \varepsilon}{k^2}. \tag{8}$$

We only consider C_μ values in the range of $y^+ > 50$, a condition in which C_μ, in average, remains constant [5]. Fluctuation of C_μ about this average is modeled by a Weibull distribution [18] with shape $\alpha_w = 45.54$ and scale parameter $\beta_w = 8.77 \times 10^{-2}$. The Weibull distribution is given by

$$f(x) = \frac{\alpha_w}{\beta_w} \left(\frac{x}{\beta_w} \right)^{\alpha_w - 1} \exp\left[-\left(\frac{x}{\beta_w} \right)^{\alpha_w} \right]. \tag{9}$$

$C_{\varepsilon 2}$ seen in Eq. (2) is the next coefficient for which a PDF is assigned. Experimental values reported by Mohamed and LaRue [19] for a gird-generated decaying homogenous turbulence are used to construct the PDF for this coefficient. Specifically, the decay factor data found in their experiment is utilized to obtain values for $C_{\varepsilon 2}$. For decaying homogenous turbulence Eqs. (1) and (2) are, respectively, simplified to

$$\frac{dk}{dt} = P - \varepsilon, \tag{10}$$

and

$$\frac{d\varepsilon}{dt} = C_{\varepsilon 1} \frac{P\varepsilon}{k} - C_{\varepsilon 2} \frac{\varepsilon^2}{k}. \tag{11}$$

When considering no velocity gradients, the production is zero and the turbulence decays. The $k-\varepsilon$ equations take the form

$$k(t) = k_0 \left(\frac{t}{t_0} \right)^{-n}, \tag{12}$$

and

$$\varepsilon(t) = \varepsilon_0 \left(\frac{t}{t_0} \right)^{-n+1}, \tag{13}$$

where k_0 and ε_0 are the turbulence kinetic energy and dissipation rate, respectively, at a reference time t_0

$$t_0 = n \frac{k_0}{\varepsilon_0}. \tag{14}$$

The decay exponent n is

$$n = \frac{1}{C_{\varepsilon 2} - 1}. \tag{15}$$

By rearranging, $C_{\varepsilon 2}$ is obtained as

$$C_{\varepsilon 2} = \frac{n+1}{n}. \tag{16}$$

Using the data from the experimental values for the decay exponent reported by Mohamed and LaRue [19], the value for $C_{\varepsilon 2}$ can be derived. The experimental reported values are seen to yield a nominal value of 1.77; however, it has been shown that $C_{\varepsilon 2} = 1.92$ yields better results [5]. The distribution is appropriately adjusted to yield a mean value of 1.92. Parameters associated with this distribution are $A_1 = 1.61$, $A_2 = 2.49$, $p = 4.21$, and $q = 7.66$.

The uncertainty in $C_{\varepsilon 1}$ utilized in Eq. (2) is determined through its relation to the model coefficient $C_{\varepsilon 2}$. Pope [5] discusses the relation based on the experimental observations made in the homogeneous shear flow. According to these observations the Reynolds stresses are self-similar in the homogenous shear flow. Therefore, the non-dimensional parameters of Sk/ε and P/ε become constant for a constant mean shear rate S. As a consequence of this constancy one obtains

$$\frac{d}{dt}\left(\frac{k}{\varepsilon}\right) = \frac{d\tau}{dt} = (C_{\varepsilon 2} - 1) - (C_{\varepsilon 1} - 1)\left(\frac{P}{\varepsilon}\right). \tag{17}$$

As stated by Pope [5] the model predicts that τ remains constant for a particular value of P/ε. This value is

$$\frac{P}{\varepsilon} = \frac{C_{\varepsilon 2} - 1}{C_{\varepsilon 1} - 1} \approx 2.1. \tag{18}$$

It is seen in this equation that $C_{\varepsilon 1}$ is correlated to $C_{\varepsilon 2}$ and can be expressed as

$$C_{\varepsilon 1} = \frac{1}{\left(\frac{P}{\varepsilon}\right)^{k-\varepsilon}} C_{\varepsilon 2} + \frac{\left(\frac{P}{\varepsilon}\right)^{k-\varepsilon} - 1}{\left(\frac{P}{\varepsilon}\right)^{k-\varepsilon}}. \tag{19}$$

Having sampled $C_{\varepsilon 2}$ via the LHS, $C_{\varepsilon 1}$ is calculated from this correlation for each sample.

The model coefficient σ_k in Eq. (1), which is considered as the 'turbulent Prandtl number' for kinetic energy, in general, is set to $\sigma_k = 1$ [5]. There has been no data available in the literature in order to estimate a PDF for this coefficient. So in an ad hoc manner we use a normal distribution with $\mu = 1.00$ and $\sigma = 1.67 \times 10^{-2}$ for this parameter.

The PDF for σ_ε in Eq. (2) is determined by observing the behavior of the flow in the log-law region and assuming a high Reynolds-number flow in a fully developed channel flow. U, k, and ε quantities are solely dependent on y so k and ε equations, respectively, simplify to

$$0 = \frac{d}{dy}\left(\frac{\nu_T}{\sigma_k}\frac{dk}{dy}\right) + P - \varepsilon, \tag{20}$$

and

$$0 = \frac{d}{dy}\left(\frac{\nu_T}{\sigma_\varepsilon}\frac{d\varepsilon}{dy}\right) + C_{\varepsilon 1}\frac{P\varepsilon}{k} - C_{\varepsilon 2}\frac{\varepsilon^2}{k}. \tag{21}$$

In the log-law region $P = \varepsilon = u_\tau^3/\kappa y$ [5]; therefore, the diffusion term is zero implying a uniform k. The equality of P and ε in ε equation results in a net sink equal to $-(C_{\varepsilon 2} - C_{\varepsilon 1})\varepsilon^2/k$ that varies as y^{-2}. The net sink is balanced by the diffusion of ε away from the wall and the ε equation is satisfied by the relation

$$\varepsilon = \frac{{C_\mu}^{3/4}\kappa^{3/4}}{\kappa y}, \tag{22}$$

leading to the following correlation for the constants

$$\kappa^2 = \sigma_\varepsilon {C_\mu}^{1/2}\left(C_{\varepsilon 2} - C_{\varepsilon 1}\right). \tag{23}$$

Thus, using this equation σ_ε can be calculated from κ, C_μ, and $C_{\varepsilon 2}$ for each sample of LHS.

The PDF of the wall function constant κ is found using the log-law relation in Eq. (6). The commonly used values for the parameters in Eq. (6) are $\kappa = 0.41$ and $B = 5.20$ determined from the DNS performed by Kim et al. [17] in a turbulent channel flow. There is some variation in literature for the experimental values

Table 1. Turbulence Model Coefficients Distributions.

C_μ	Weibull	$\alpha_w = 45.54$ and $\beta_w = 8.77 \times 10^{-2}$
$C_{\varepsilon 2}$	beta	$A_1 = 1.61, A_2 = 2.49,$
		$p = 4.21, q = 7.66$
σ_k	normal	$\mu = 1.00$ and $\sigma = 1.67 \times 10^{-2}$
κ	normal	$\mu = 0.41$ and $\sigma = 4.89 \times 10^{-3}$
B	normal	$\mu = 5.20$ and $\sigma = 0.10$

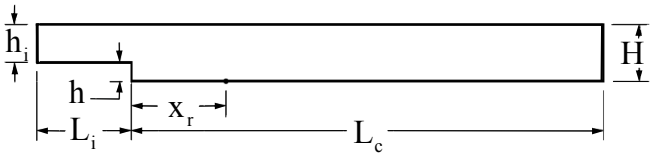

Figure 1. BACKWARD-FACING STEP GEOMETRY.

for these parameters, but most authors agree within 5% of these values. The log-law relation Eq. (6), in the region $y^+ > 30$, is used to obtain the PDF for κ. In order to do so, the mean value for the smoothness parameter $B = 5.20$ is held constant and the data for κ is taken from the numerical data reported by Kim *et al.* [17]. As a result, the PDF for κ is determined to be a normal distribution with $\mu = 0.41$ and $\sigma = 4.89 \times 10^{-3}$.

The PDF of the wall function parameter B is also obtained using the log-law relation Eq. (6) and the reported data of Kim *et al.* [17]. κ is set to 0.41, with the same restriction of $y^+ > 30$, and then the values for the parameter B are obtained. The PDF for B is set to a normal distribution $\mu = 5.20$ and $\sigma = 0.10$.

Table 1 summarizes the PDFs considered for three coefficients of the $k-\varepsilon$ model, the wall function parameters, and turbulence intensity. We recall that model coefficient $C_{\varepsilon 1}$ not tabulated in this table, depends on $C_{\varepsilon 2}$ and can be calculated from Eq. (19) for each sample. σ_ε, the other model coefficient which is not tabulated in the table either, can be calculated through Eq. (23) in terms of κ, C_μ, $C_{\varepsilon 1}$ and $C_{\varepsilon 2}$ for each sample.

We also consider uncertainty in the value turbulence intensity at the inlet boundary with a mean of 5% of the mean inlet velocity U. The considered PDF for I_T is a normal distribution with $\mu = 0.05$ and $\sigma = 8.33 \times 10^{-4}$.

BACKWARD-FACING STEP FLOW

We conduct our study for a turbulent flow over a backward-facing step displayed in Fig. 1. This configuration is considered as an important benchmark problem for testing new developments in the area of CFD as it provides valuable information useful to many practical situations. This is due to the fact that many actual flow situations are characterized by the flow separation of the boundary layer and the subsequent reattachment of the flow downstream, which is a flow structure also seen in the backward-facing step. In this study, the step expansion ratio defined as step height to outlet channel height is $h/H = 1/3$ (Fig. 1). The values used in this study for the channel lengths are $L_i = 5h$ and $L_c = 30h$. It has been shown that these values are large enough so that they do not influence the main flow structure [20]. The dimensions of the backward-facing step configuration used in our study is the same as that in the experimental study of Kim *et al.* [21]. The Reynolds number based on the inlet centerline velocity and the outlet channel height is $Re_H = 132000$.

The process of quantifying the uncertainties is done by utilizing the LHS technique in order to obtain a smaller number of sample setups for the CFD analysis. The uncertainties in the $k-\varepsilon$ model coefficients along with the wall function parameters and turbulence intensity are found by sampling from their individual PDFs. We set the number of samples in the current study to 100. Each sample is run by an open source CFD software, *OpenFOAM*, a product of the commercial company OpenCFD Ltd. Using this software and accounting for no uncertainties, we have been able to regenerate results obtained by another study [22] on the same backward-facing step we consider. The study reported in [22] has found that a finite-volume method with a 200×100 unstructured mesh yields results within 0.3% of the grid independent solution. We have used the same resolution for all LHS samples required for the uncertainty quantification.

RESULTS

Fig. 2 shows the profiles of the velocity component at x direction at various locations past the backward-facing step. The mean streamwise velocities are normalized by the inlet velocity. The mean velocity profiles are indicative of the expected characteristics for flow over the backward-facing step and compare well with the experimental results obtained by Kim *et al.* [21]. The uncertainty appears to be the largest in the recirculation region and closer to the bottom wall specifically near the reattachment point. The recirculation region is characterized by the primary large recirculating eddy, alternating the orientation of streamwise velocities. At the reattachment point the streamwise velocity returns to a positive orientation and downstream of this point returns to a boundary layer flow. Close to the bottom wall in Fig. 2d, where the velocity profiles are displayed at $x = 5.33$ and $x = 6.22$ which are very close to the location of the reattachment point, the largest level of uncertainty of the streamwise velocity component is observed.

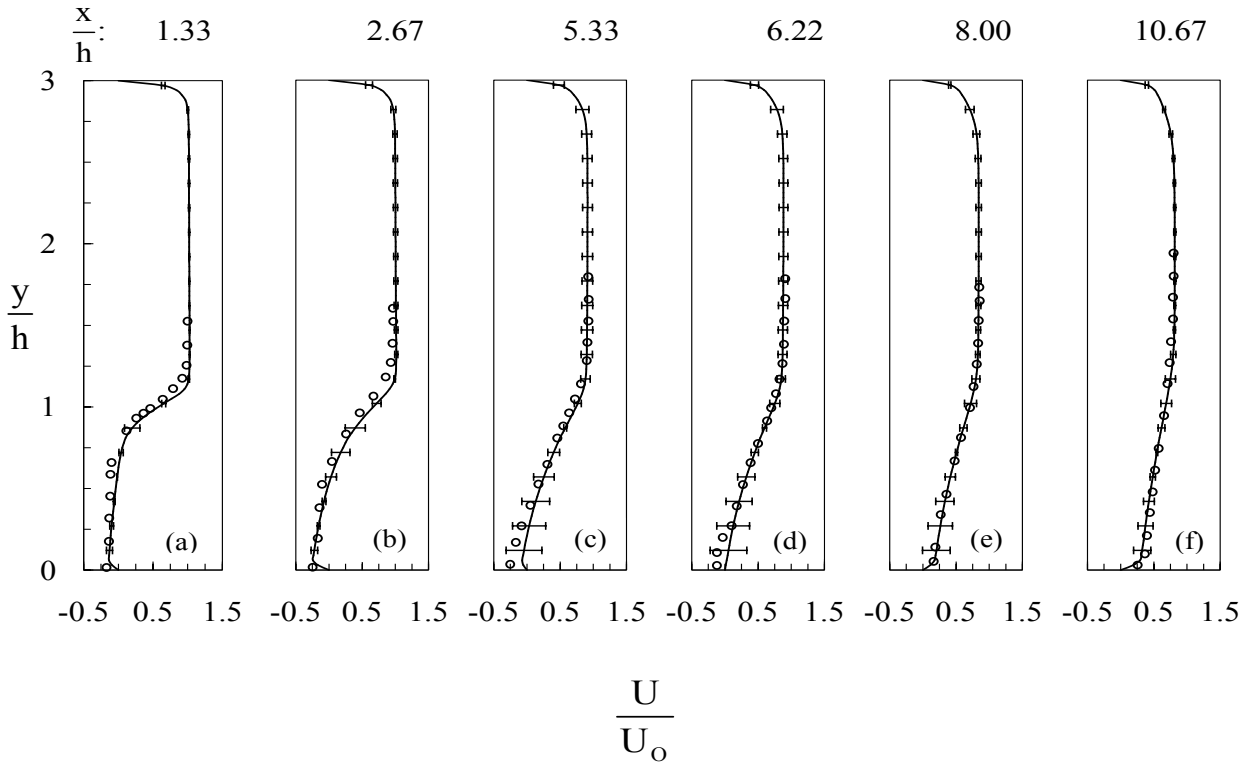

Figure 2. STREAMWISE VELOCITY PROFILES WITH 6σ UNCERTAINTY ERROR BARS (— COMPUTATIONS; O EXPERIMENTS OF KIM *et al.*, 1987).

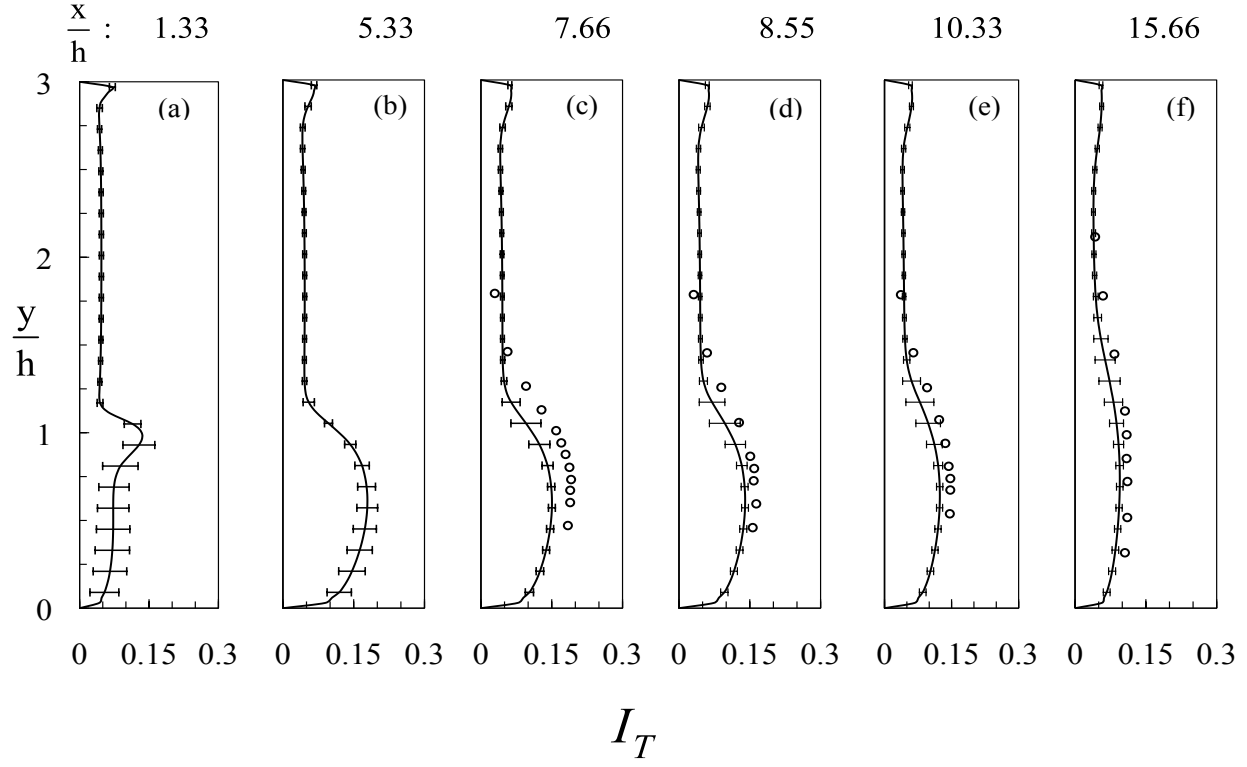

Figure 3. TURBULENCE INTENSITY PROFILES WITH 6σ UNCERTAINTY ERROR BARS (— COMPUTATIONS; O EXPERIMENTS OF KIM *et al.*, 1987).

The profiles of the nondimensional turbulence intensity defined by $I_T = \sqrt{u'u'}/U_0$, where u' is the turbulence fluctuation of the the velocity component at x direction, are shown in Fig. 3 at selected locations past the step. The turbulence intensities are also normalized by the inlet velocity. The comparison between computational and experimental values of the turbulence intensity seen in Figs. 3c and 3d reveals good agreement between them slightly deviating closer to the reattachment point in the recirculating zone. The spatial variation of uncertainty in the value of the computed turbulence intensity along y direction is observed in Fig 3 to be a strong function of the x locations where the profiles are displayed. Uncertainty in the turbulence intensity seems to be the largest in the recirculation region as seen in Fig. 3(a) and (b). Specifically, uncertainty is much larger in a region limited between $y = 0$ and $y/h \approx 1$ than that for other values of y. However, further downstream seen in Figs. 3c through 3f, the region with high uncertainty in the value of turbulence intensity is shifted towards the core flow in the channel.

Figs. 4a and 4b show the spatial variation of the static pressure normal to the surface represented by the wall pressure coefficient along with its uncertainty at the top and bottom walls past the step, respectively. The pressure coefficient is defined by

$$C_p = \frac{2(P - P_0)}{\rho {U_0}^2}, \tag{24}$$

where P_0 and U_0 denote the centerline pressure and velocity at the channel inlet, respectively. The mean pressure coefficient profiles compare well with the experimental results obtained by Kim *et al.* [21]. The uncertainty in the pressure coefficients seems to be the largest in the vicinity of the reattachment point on both top and bottom walls. Interestingly, the uncertainty in the value of C_P vanishes downstream of the flow on both top and bottom walls.

The wall shear stress can be seen in Fig. 5 at selected locations along the bottom wall past the step. The wall shear stress is defined by

$$\tau_w = \mu_f \left.\frac{\partial U}{\partial y}\right|_{y=0}. \tag{25}$$

Also, the dimensionless form of the wall shear stress C_f is defined by

$$C_f = \frac{2\tau_w}{\rho {U_0}^2}. \tag{26}$$

Fig. 5 shows C_f/C_{fout}, where C_{fout} denotes C_f at the fully developed outlet, plotted against the normalized distances $(x - x_r)/x_r$ [23]. The wall shear ratio profile is compared to the experimental values obtained by Driver and Seegmiller [24] who conduct their study for an expansion ratio of $h/H = 1/9$ and obtain a reattachment point of $x_r/h = 6.26$. Their experimental results are scaled and then compared to our numerical results. The uncertainty in the wall shear stress ratio along the bottom wall is shown to be also the largest in the vicinity of the reattachment point; however, it does not taper as much as the pressure coefficient does. It maintains significant uncertainty in its value fully downstream.

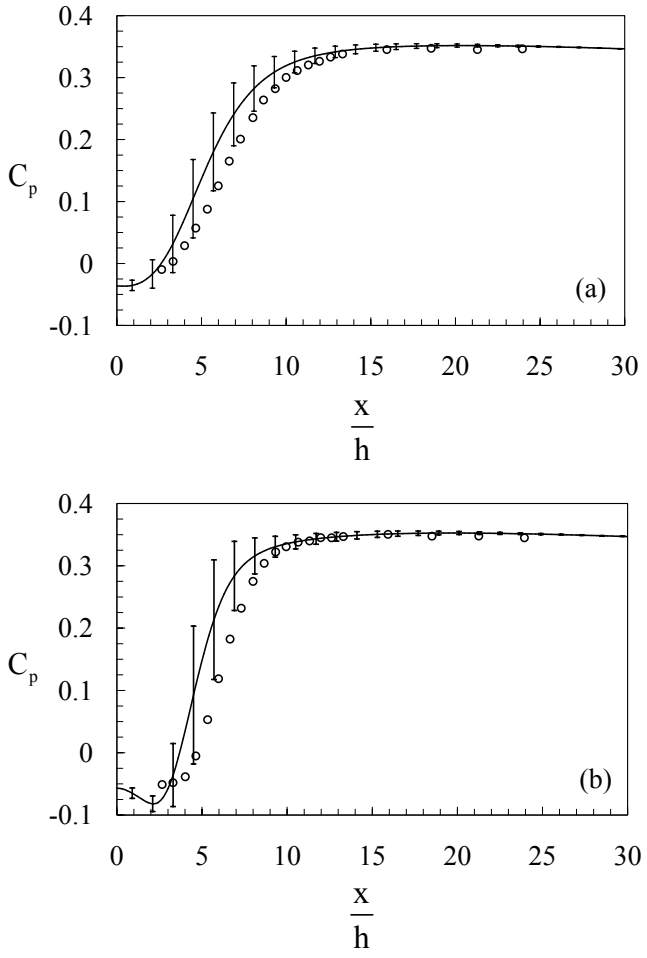

Figure 4. PRESSURE COEFFICIENT ALONG THE (a) TOP WALL AND (b) BOTTOM WALL WITH 6σ UNCERTAINTY ERROR BARS (— COMPUTATIONS; O EXPERIMENTS OF KIM *et al.*, 1987).

Because of the importance of the location of the reattachment point, the variation of the reattachment point is also investigated. The reattachment point is found by locating the point where the wall shear stress becomes exactly zero. This is done by determining the point where the streamwise velocity component adjacent to the wall is changing its orientation from nega-

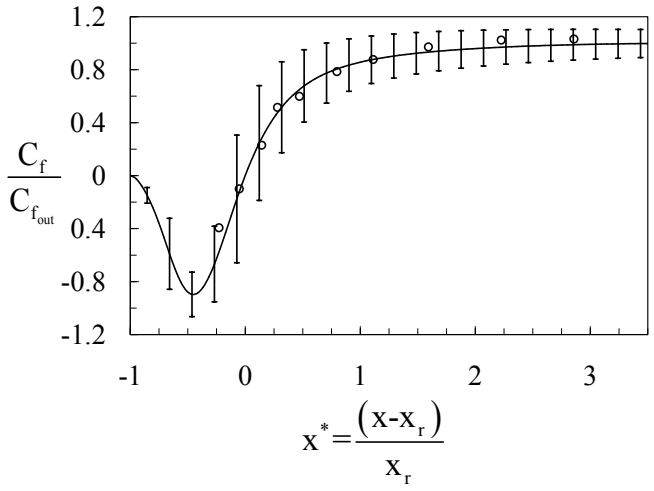

Figure 5. SHEAR STRESS ALONG THE BOTTOM WALL WITH 6σ UNCERTAINTY ERROR BARS (— COMPUTATIONS; O EXPERIMENTS OF DRIVER & SEEGMILLER, 1985).

tive to positive [25]. It is known that the standard $k-\varepsilon$ model underpredicts the reattachment length by about 20% [26]. For this reason, many have tuned the model coefficients in order to obtain a better prediction of the reattachment point. Fig. 6 shows the histogram as well as $f(x_r)$, the PDF of the location of the reattachment point. Predicted by *EasyFit*, $f(x_r)$ is a lognormal distribution with $\mu_l = 1.82$ and $\sigma_l = 0.070$. A lognormal distribution is defined by

$$f(x) = \frac{1}{x\sigma_l\sqrt{2\pi}} \exp\left[\frac{-(\ln x - \mu_l)^2}{2\sigma_l^2}\right], \qquad (27)$$

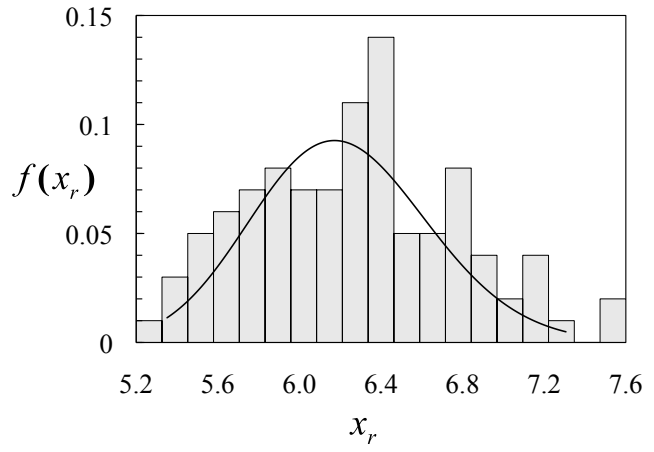

Figure 6. PDF OF THE LOCATION OF REATTACHMENT POINT.

where μ_l and σ_l are the mean and standard deviations of the variable's natural logarithm [18].

SUMMARY AND CONCLUSION

A study of the inherent uncertainties in the turbulence model coefficients and parameters was the focus of this work. Specifically, this study sets out to quantify the uncertainties in the coefficients and parameters of the standard $k-\varepsilon$ turbulence model via the Latin Hypercube Sampling method. We have been able to statistically describe the variability of the input parameters of interest and observe the effects that they incur on the output flow parameters. The sampling of uncertainties of the input parameters has been carried out by the LHS method which greatly reduces the number of required samples compared to conventional Monte-Carlo methods.

The standard $k-\varepsilon$ turbulence model has been applied to the well documented configuration of the 2D backward-facing step for which there are experimental results available. While for flow variables of interest such as velocities at various locations computed average values from CFD outputs are compared against their experimental counterparts in the figures, their standard deviations are also displayed using error bars. The highest uncertainties seem to occur in the recirculation region and near the reattachment point for most of the outputs. The results of this work provide evidence that minimal variations of the standard $k-\varepsilon$ model input coefficients and parameters, may yield significant uncertainties in the flow variables in the backward-facing step.

ACKNOWLEDGMENT

The authors acknowledge Gregory D. Wyss of Sandia National Laboratories for his instruction on installing and using the LHS software.

REFERENCES

[1] Faragher, J., 2006. The Implementation of Probabilistic Methods for Uncertainty Analysis in Computational Fluid Dynamics Simulations of Fluid Flow and Heat Transfer in a Gas Turbine Engine. Tech. Rep. DSTO-TR-1830, Defense Science and Technology Division, Victoria, Australia.

[2] Platteeuw, P., Loeven, G., and Bijl, H., 2008. "Uncertainty Quantification Applied to the k - ε Model of Turbulence Using the Probabilistic Collocation Method". In AIAA Structures, Structural Dynamics, and Material Conference.

[3] Lucor, D., Meyers, J., and Sagaut, P., 2007. "Sensitivity analysis of large-eddy simulations to subgrid-scale-model parametric uncertainty using polynomial chaos". *Journal of Fluid Mechanics,* **585** , pp. 255–279.

[4] Jouhaud, J.-C., Sagaut, P., Enaux, B., and Laurenceau, J., 2008. "Sensitivity analysis and multiobjective optimization for les numerical parameters". *Journal of Fluids Engineering,* **130** , p. 021401.

[5] Pope, S. B., 2000. *Turbulent Flows*. Cambridge University Press, Cambridge, UK.

[6] Jones, W., and Launder, B., 1972. "The Prediction of Laminarization with a Two-Equation Model of Turbulence". International Journal of Heat and Mass Transfer, **15** (2) , pp. 301–314.

[7] Habib, N., 2009. "Uncertainty Quantification and Polynomial Chaos Techniques in Computational Fluid Dynamics". *Annual Review of Fluid Mechanics,* **41** , pp. 35–52.

[8] McKay, M., Beckman, R., and Conover, W., 1979. "A Comparison of Three Methods for Selecting Values of Input Variable in the Analysis of Output from a Computer Code". Technometrics, **21** (2) , pp. 239–245.

[9] Iman, R., Helton, J., and Campbell, J., 1981. "An Approach to Sensitivity Analysis of Computer Models, Part 1. Introduction, Input Variable Selection and Preliminary Variable Assessment". Journal of Quality Technology, **13** (3) , pp. 174–183.

[10] Helton, J., and Davis, F., 2003. "Latin Hypercube Sampling and the Propagation of Uncertainty in Analyses of Complex Systems". Reliability Engineering and System Safety, **81** (1) , pp. 23–69.

[11] Stein, M., 1987. "Large Sample Properties of Simulations Using Latin Hypercube Sampling". Technometrics, **29** (2) , pp. 143–151.

[12] Wyss, G., and Jorgensne, K., 1998. A User's Guide to LHS: Sandia's Latin Hypercube Sampling Software. Tech. Rep. SAND98-0210, Risk Assessment and Systems Modeling Department, Sandia National Laboratories, Albuquerque, NM.

[13] Cheng, J., and Druzdel, M., 2000. "Latin Hypercube Sampling in Bayesian Networks". In Proceedings of the 13th International Florida Artificial Intelligence Research Symposium Conference, pp. 287–292.

[14] Von Kármán, T., 1930. "Mechanische Ähnlichkeit und Turbulenz". In Proceedings of the Third International Congress of Applied Mechanics, pp. 85–105.

[15] Launder, B., and Sharma, B., 1974. "Application of Energy-Dissipation Model of Turbulence to the Calculation of Flow Near a Spinning Disc". *Letters in Heat and Mass Transfer,* **1** , pp. 131–138.

[16] Dekking, F., Kraaikamp, C., Lopuhaa, H., and Meester, L., 2005. *A Modern Introduction to Probability and Statistics*. Springer, Delft University of Technology.

[17] Kim, J., Moin, P., and Moser, R., 1987. "Turbulence Statistics in Fully Developed Channel Flow at Low Reynolds Number". *Journal of Fluid Mechanics,* **177** , pp. 133–166.

[18] Swiler, L. P., and Wyss, G. D., 2004. A User's Guide to LHS: Sandia's Latin Hypercube Sampling Software: LHS UNIX Library/Standalone Version. Tech. Rep. SAND2004-2439, Sandia National Laboratories, Albuquerque, NM.

[19] Mohamed, M., and Larue, J., 1990. "The Decay Power Law in Grid-Generated Turbulence". *Journal of Fluid Mechanics,* **219** , pp. 195–214.

[20] Biswas, G., Breuer, M., and Durst, F., 2004. "Backward-Facing Step Flows for Various Expansion Ratios at Low and Moderate Reynolds Numbers". *Journal of Fluids Engineering,* **126** , pp. 362–374.

[21] Kim, J., Kline, S., and Johnston, J., 1980. "Investigation of a Reattaching Turbulent Shear Layer: Flow Over a Backward-Facing Step". *ASME Journal of Fluids Engineering,* **102** , pp. 302–308.

[22] Thangam, S., and Hur, N., 1991. "A Highly-Resolved Numerical Study of Turbulent Separated Flow Past a Backward-Facing Step". International Journal of Engineering Science, **29** (5) , pp. 607–615.

[23] Adams, E., and Eaton, J., 1988. "An LDA study of the Backward-Facing Step Flow, Including the Effects of Velocity Bias". *ASME Journal of Fluids Engineering,* **110** , pp. 275–282.

[24] Driver, D., and Seegmiller, H., 1985. "Features of a Reattaching Turbulent Shear Layer in Divergent Channel Flow". *AIAA Journal,* **23** , pp. 163–171.

[25] Nie, J., and Armaly, B., 2003. "Reattachment of Three Dimensional Flow Adjacent to Backward-Facing Step". Journal of Heat Transfer, **125** (3) , pp. 422–428.

[26] Thangam, S., and Speziale, C., 1991. Turbulent Separated Flow Past a Backward-Facing Step: A Critical Evaluation of Two-Equation Turbulence Models. Tech. Rep. ICASE Report No. 91-23, NASA Langley Research Center, Langley, Virginia.